Supporting Information

Title:

Monolayer Effect of a Gemini Surfactant with a Rigid Biphenyl Spacer on its Self-crystallization at the Air/liquid Interface

Authors:

Qibin Chen, Junyao Yao, Xin Hu, Jincheng Shen, Yujie Sheng, Honglai Liu

Affiliations:

Department of Chemistry, East China University of Science and Technology, Shanghai, 200237, China

E-mail: hlliu@ecust.edu.cn.

Contents:

Density Functional Theory (DFT) Computational methods

The complexes studied in this work were computed at the M06/6-31+G(d) level of theory by means of the Gaussian 09 package using the crystallographic coordinates[1]. These complexes were carefully selected to represent all relevant interactions in solid state as well as to have a neutral charge. The interaction energy is defined as follows:

$$\Delta E = E(\text{complex}) - \sum E(\text{monomer}) \quad (1)$$

where E(complex) is the total energy of the complex, and $\sum E$(monomer) is the sum of the total energy of the monomers.

Characterization Data

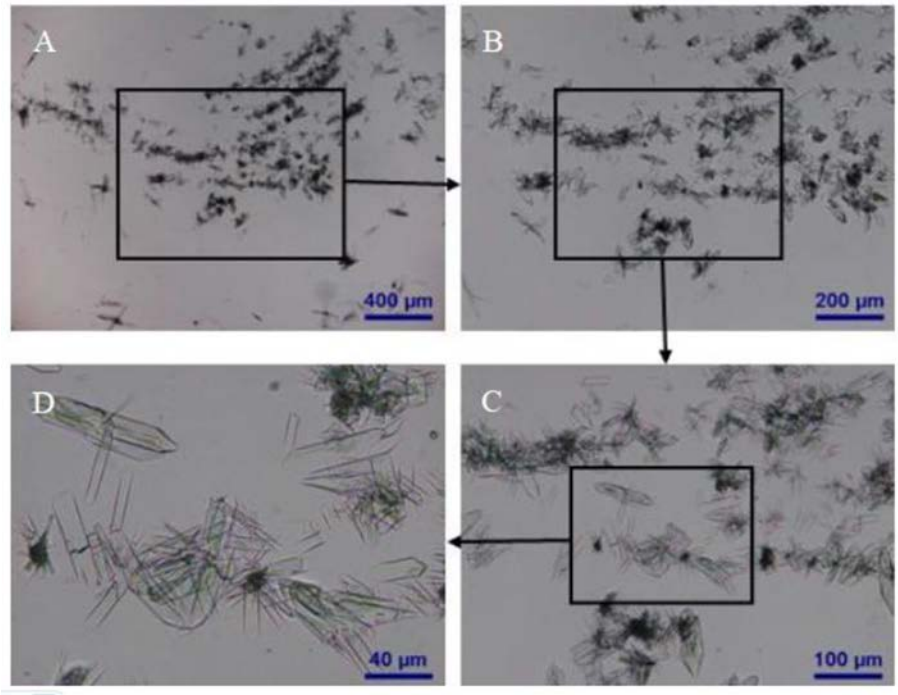

Figure S1. OM images of 12-2Ar crystal aging after a short period of time (~1hour). The magnification of the objective lense A: (5×), B: (10×), C: (20×), D: (50×)

Figure S1A gives the overall view of the interfacial crystal of 12-2Ar obtained after a short aging period of ~1 hour. The crystal appearance seems to be irregular. However, the higher magnification images (Figure S1C and D) reveal that most of the 12-2Ar crystals display sword strips. Furthermore, there are many aggregated sword strips and a small quantity of individual sword strips, indicating that sword strips apparently experience an aggregation process, which can be further illustrated by Figure S2.

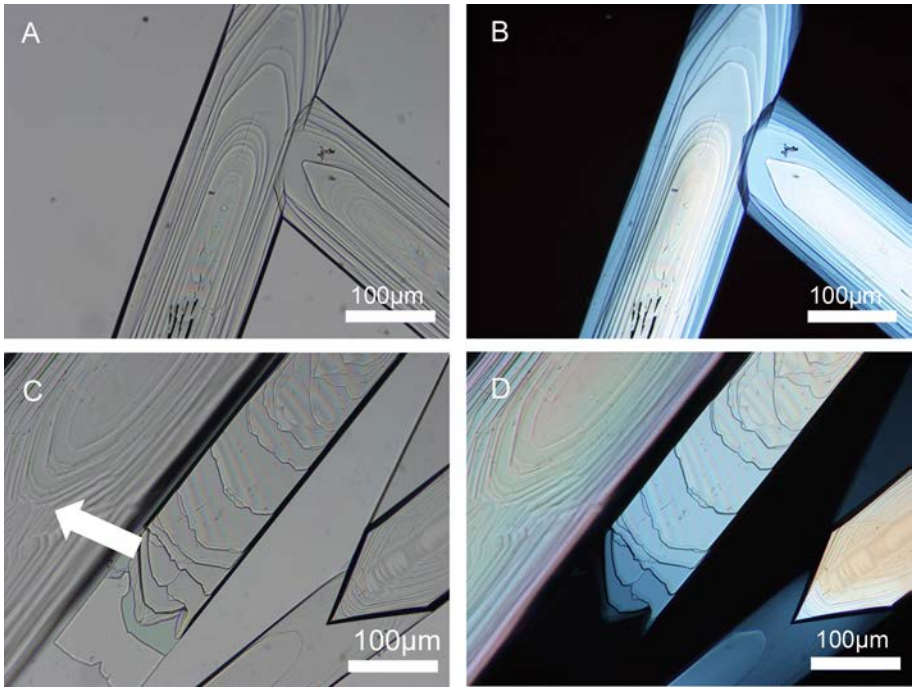

Figure S2. Wrapping phenomena and longitudinal growth among the sword strips during the 12-2Ar crystal growth. A: OM, B: POM, C: OM, D: POM

Fortunately, the wrapping phenomena of the sword strips were observed by optical microscope and SEM in the course of the crystal growth. In Figure S2A and B, the end of one strip commences only clamping the side of the other. In Figure S2C and D, two strip crystals grow along the longitudinal direction and form a joint, indicated by arrow.

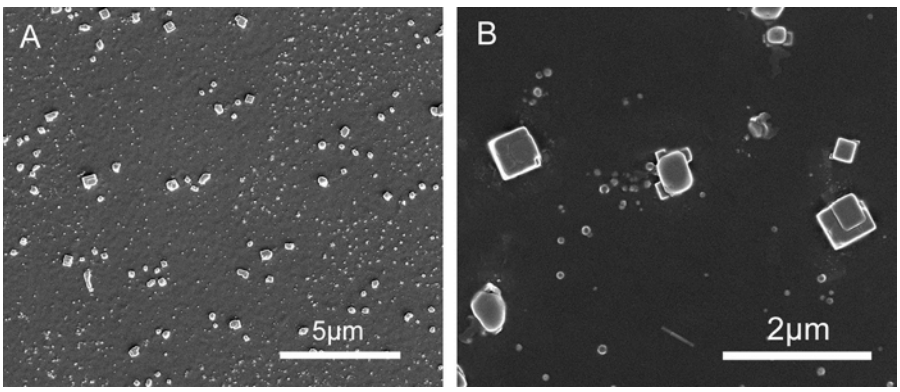

Figure S3. SEM images of 12-2Ar crystals at the aging time of 30 minutes

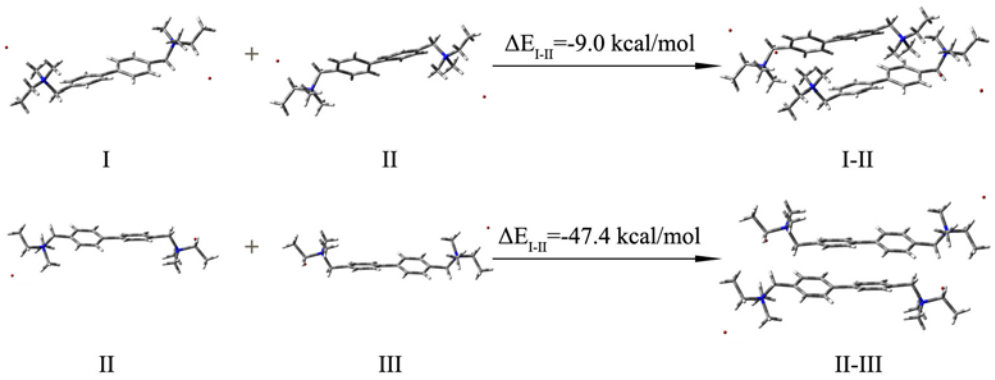

Figure S4. The interactions of biphenyl and/or head groups between the neighboring molecules according to DFT calculations.

A computational study using DFT calculations has been performed to analyze noncovalent interactions in the neighboring molecules along *c* axis. The calculated interaction energies between the neighboring molecules along *c* axis are shown in Figure S4. It can be seen that the interaction energy of the system that contains I, II and III is quite large (-56.4 kcal/mol), which is contributed by the interaction energy of a molecular pair (ΔE_{I-II} = -9.0 kcal/mol) and two neighboring molecules belonging to different molecular pairs (ΔE_{II-III} = -47.4 kcal/mol). Clearly, the interaction energy between the neighboring molecules is mainly ascribed to cation-π interaction between quaternary ammonium and benzene and π-π stacking interaction between the adjacent biphenyls.

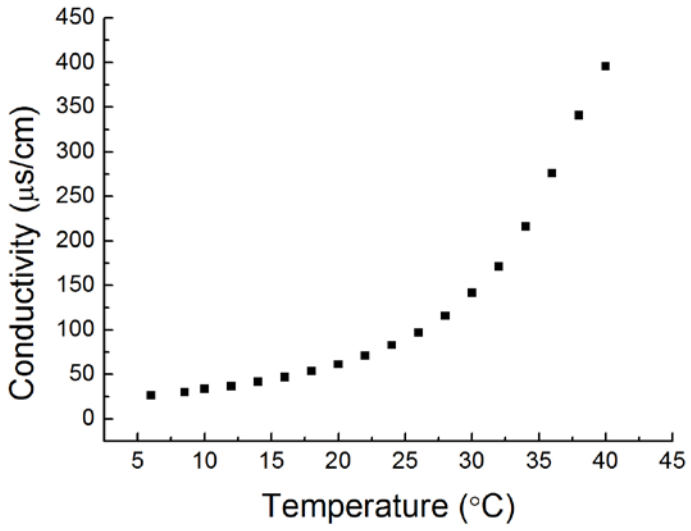

Figure S5. The variation of conductivity of 12-2Ar solution with temperature.

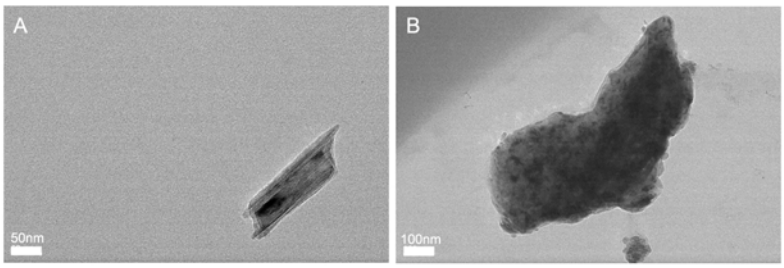

Figure S6. TEM images of aggregates obtained at the air/water interface. A: regular structure; B: irregular structure.

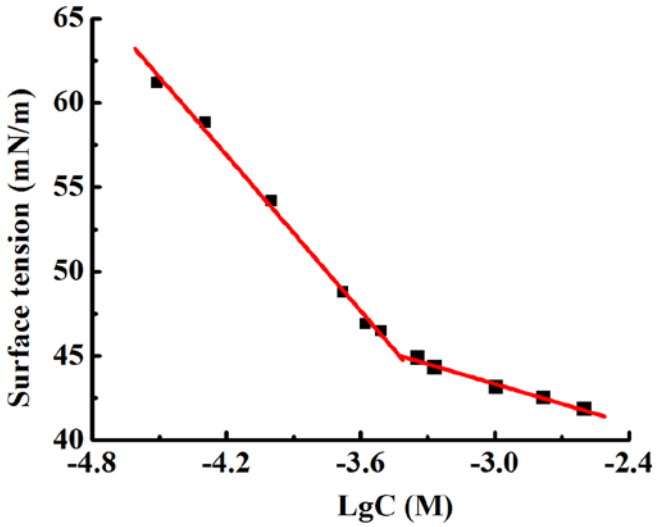

Figure S7. Equilibrium surface tension versus log bulk surfactant concentration of 12-2Ar in water at 23.0 °C. CMC of 12-2Ar is 0.374mM, γ_{CMC} =45.01mN/m.

Surface tension measurements of 12-2Ar solutions were measured by the automated pendant drop method on the interface rheometer. As for surface tension measurements, equilibrium was considered to be obtained when a stable value was approaching. Equilibrium surface tension, γ_s, versus log bulk surfactant concentration of 12-2Ar in water at 23.0 °C is plotted in Figure S7. The surface excess concentration, Γ, and the minimum area per molecule, A_{min}, were calculated using the Gibbs equation as follows:

$$\Gamma = -\frac{1}{2.303nRT}\frac{d\gamma}{d\lg C}$$

$$A_{min} = \frac{1}{N_A\Gamma}\times 10^{16}$$

where R = 8.314 J·mol^{-1}K^{-1}, N_A = Avogadro's number, Γ is in mol·cm^{-2}, and A_{min} is in (nm^2·molecule^{-1})

$\times 10^2$. The parameter *n* represents the number of species at the interface whose concentration changes with surfactant concentration. It must be pointed out that *n* is not explicitly defined. For cationic surfactants, its value is unambiguous only in the presence of a swamping amount of electrolyte. Under these conditions *n* = 1. For a uni-univalent ionic surfactant in water the value n = 2 is generally used. In a gemini aqueous solution, it has been set at 2 or 3 by various investigators[2]. Here, A_{min} of 12-2Ar is equal to 1.83 and 1.22 $nm^2 \cdot molecule^{-1}$ when n = 2 and 3, respectively. At present, *n* = 3 is more acceptable, thus this value is chosen in this study. The resulting A_{min} is equal to 1.83 $nm^2 \cdot molecule^{-1}$. Menger et al. have systematically investigated the solution and interface behaviors of geminis with rigid spacers and proposed that they lie absolutely horizontally at the air/water interface[3-5]. The rigid spacer forces the two chains to separate and has a significant effect on the molecular orientation. They had come to the conclusion that only with sufficient film pressure (ca. 34 mN/m), it is possible to reorient both horizontal chains of gemini with rigid spacer into a vertical arrangement, which was confirmed by our previous work[6].

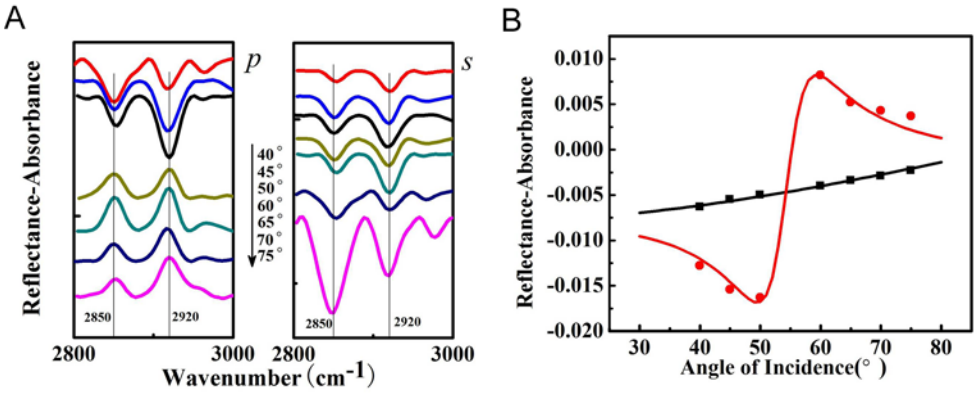

Figure S8. IRRAS spectrum of SA (A) and the corresponding comparison of simulated (red and black line for *p*- and *s*- polarizations respectively) lines and measured $v_s(CH_2)$ (solid circles and square symbols for *p*- and *s*-polarizations respectively) (B). The surface film parameters for the simulation are L=2.5nm, θ=20°, Γ=0.018, k_{max}= 0.75

In order to determine the certainty of IRRAS spectroscope, we verified the orientation of Stearic acid (SA) in the monolayer by using the same method and found the tilt angle of SA alkyl chains was close to 20º, which is consistent with that in literature[7]. Furthermore, theoretical calculations of RA lines fit quite well with the experimental values of SA. This indicates that this method used in this paper is reliable.

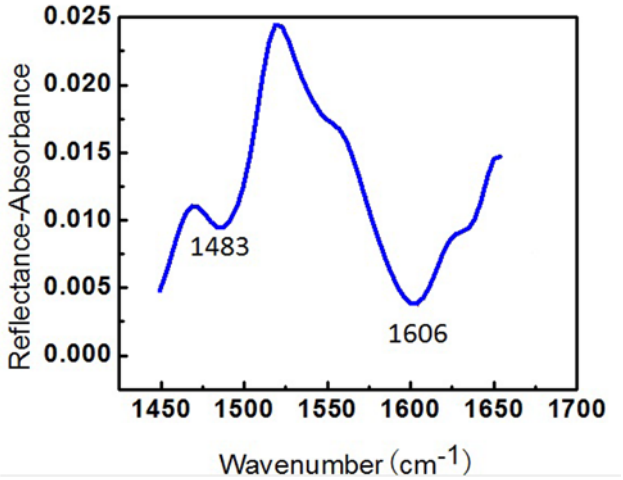

Figure S9. IRRAS spectrum of 18-2Ar monolayer at the air/water interface**.**

The aromatic ring stretching modes are present, and the most intense band at 1483 cm^{-1} is negative to the baseline, suggesting that the aromatic rings were predominantly perpendicular to the substrate surface[8].

Table S1. Single-crystal XRD data of 12-2Ar

Identification code	Interface crystal
empirical formula	$C_{42}H_{80}Br_2N_2O_3$
formula weight	820.9
temperature	140(2) K
wavelength	1.54178Å
crystal system, space group	monoclinic C 2/c
unit cell dimensions	a = 54.695(2) Åb = 9.8891(4) Åc = 16.8770(6) Å α= 90° β= 92.628(5)° γ= 90°
volume	9118.9(6) $Å^3$
Z, calculated density	8, 1.196 Mg/m^3
absorption coefficient	2.517 mm^{-1}
F(000)	3520
θ range for data collection	1.62 to 64.00°
limiting indices	-63<=h<=62, -11<=k<=11, -15<=l<=19
data/restraints/parameters	7273/65/448
goodness-of-fit on F2	1.172
final R indices [I > 2σ(I)]	R1 = 0.1241, wR2 = 0.3079
R indices (all data)	R1 = 0.1484, wR2 = 0.3304
CCDC number	1031724

References

[1] Gaussian 09 (Revision A.1), M. J. Frisch, G. W. H. Trucks, B. Schlegel, G. E. Scuseria, M. A. Robb, J. R. Cheeseman, G. Scalmani, V. Barone, B. Men-nucci, G. A. Petersson, H. Nakatsuji, M. Caricato, X. Li, H. P. Hratchian, A. F. Izmaylov, J. Bloino, G. Zheng, J. L. Sonnenberg, M. Hada, M. Ehara, K. Toyota, R. Fukuda, J. Hasegawa, M. Ishida, T. Nakajima, Y. Honda, O. Kitao, H. Nakai, T. Vreven, J. A. Montgomery, J. E. Peralta, Jr. , F. Ogliaro, M. Bearpark, J. J. Heyd, E. Brothers, K. N. Kudin, V. N. Staroverov, R. Ko-bayashi, J. Normand, K. Raghavachari, A. Rendell, J. C. Burant, S. S. Iyen-gar, J. Tomasi, M. Cossi, N. Rega, J. M. Millam, M. Klene, J. E. Knox, J. B. Cross, V. Bakken, C. Adamo, J. Jaramillo, R. Gomperts, R. E. Stratmann, O. Yazyev, A. J. Austin, R. Cammi, C. Pomelli, J. W. Ochterski, R. L. Martin, K. Morokuma, V. G. Zakrzewski, G. A. Voth, P. Salvador, J. J. Dannenberg, S. Dapprich, A. Daniels, D. Farkas, J. B. Foresman, J. V. Ortiz, J. Cio-slowski, D. J. Fox, *Gaussian, Inc.*, Wallingford, CT, **2009**.

[2] R. Zana, *Adv. Colloid Interface Sci.*, **2002**, *97*, 205-253.

[3] F. M. Menger, C. A. Littau, *J. Am. Chem. Soc.*, **1993**, *115*, 10083-10090.

[4] F. M. Menger, C. A. Littau, *J. Am. Chem. Soc.*, **1991**, *113*, 1451-1452.

[5] F.M. Menger, J. S. Keiper, *Angew. Chem. Int. Ed*., **2000**, *39*, 1906-1920.

[6] Q. B. Chen, X. D. Liang, S. L. Wang, S. H. Xu, H. L. Liu, Y. Hu, *J. Colloid Interface Sci.*, **2007**, *314*, 651-658.

[7] Y. C. Wang, X. Z. Du, L. Guo, H. J. Liu, *J. Chem. Phys*., **2006**, *124*, 134706

[8] T. Buffeteau, B. Desbat, J. M. Turlet, *Appl. Spectrosc*., **1991**, *45*, 380-389.